

COMBINED EFFECT OF SOME INTERNAL BALLISTIC PARAMETERS ON THE PRESSURE BEHAVIOR OF SOLID PROPELLANT ROCKET MOTOR

Abdulhassan A. Karamalla
Military College of Engineering – Iraq

ABSTRACT

The burning rate is an important characteristic of the solid propellant. Its sensitivity to the gas flow, parallel to the burning surface, results in a so-called "erosive burning" of the propellant. The pressure inside the combustion chamber and its maximum value is very sensitive to the change of burning rate.

This paper presents a theoretical study of the combined effect of burning rate variation and two other internal ballistic parameters which are the specific mass of solid propellant and pressure exponent upon the erosive burning phenomenon, then upon the pressure behavior inside the combustion chamber of the rocket motor.

Two main differential equations and other auxiliary algebraic equations have represented the pressure behavior from the starting of rocket motor function to the peak point (erosive peak) and its decaying from this point to the pseudo-equilibrium condition. The differential equations are solved numerically using Merson's method.

Variation of the Main Geometric Characteristics of Solid Propellant

Processes inside the combustion chamber of solid propellant rocket motor are affected by geometric characteristics of solid propellant charge. Main characteristics are: time dependence of burnt thickness $e(t)$, time dependence of the burning surface $S(t)$, and time dependence of the free volume $V_f(t)$.

The law of burning for a rocket motor can be expressed as follows:^[1,2,6]

$$u = u_0 [\exp K_T (T_P - T_N)] P_C^\alpha K_E = u_N K_E \quad (1)$$

and the burning thickness variation with time is,

$$e = ut, \text{ or}$$

$$\frac{de}{dt} = u \quad (2)$$

The instantaneous burning surface of solid propellant charge is given by the equation:

$$S = S_0 \varphi(e) \quad (3)$$

where, $\varphi(e)$ is the shape function of solid

propellant charge and can be introduced as follows:

$$\varphi(e) = 1 \pm \frac{\Delta S(e)}{S_0} \quad (4)$$

where, $\Delta S(e)$ represents the change of burning surface in terms of burnt thickness e , and the \pm sign corresponds to the real character of burning of solid propellant charge.

With respect to the fact that S_0 is not dependent upon the burnt thickness e , the main problem is the determination of $\Delta S(e)$. But e is some function time, therefore the shape function $\varphi(e)$ can be also simply transferred to $\varphi(t)$. According to the theory of solid propellant charges, the shape function $\varphi(c) \equiv \varphi(t)$ can be introduced in terms of,

$$\varphi(e) = 1 \pm a_i e \quad (5)$$

where, a_i is some constant which is a function of basic dimensions of respective geometric shape (mainly outer and inner diameter of the presupposed shape, as well as the grain length L_p).

Equation (5) can be also written in the following forms:

$$\varphi(t) = 1 \pm a_i u t$$

$$\varphi(t) = 1 \pm a_i u_0 [\exp K_T (T_P - T_N)] P_c^\alpha K_E t \quad (6)$$

or

$$\varphi(t) = 1 \pm a_i u_0 f(T_P) P_c^\alpha K_E t$$

The variation of free volume of rocket motor combustion chamber is [3,5,7]:

$$V_f = V_{f0} + \int_0^e S_0 \varphi(e) de \quad (7)$$

from which,

$$V_f = V_{f0} + S_0 u t \left[1 \pm \frac{a_i u t}{2} \right] \quad (8)$$

where, $V_{f0} = \text{constant}$, $S_0 = \text{constant}$ for a given geometric shape. The approximate value of the initial free volume is,

$$V_f = \frac{\pi}{4} \varphi_v \xi_k D^3 \bar{\theta}^2 (1 - K_f) K_L \quad (9)$$

where, [8], $K_L = \frac{L_P}{D}$.

Differential Equations of Chamber Pressure Behavior

The pressure behavior with time of burning of the solid propellant grain gives full information about internal processes inside the combustion chamber. In the present paper, the effect of some internal ballistic parameters of solid propellant on the pressure course will be studied. Mainly the effect of erosion ratio K_E , burning rate u_N , specific mass ρ_P and pressure exponent α will be discussed.

A. First period

The first period represents the pressure rise from the beginning of rocket function till the maximum value of pressure (A to B in Fig. 1). The differential equation that described this part is formulated applying the continuity equation [4,7,8],

$$\dot{m}_e = \dot{m}_N + \frac{d}{dt}(m_G) \quad (10)$$

$$\dot{m}_N = \frac{P_c A_c}{C^*} = \frac{\varphi(\gamma) P_c A_c}{(r T_c)^{0.5}} \quad (11)$$

and from equation of state,

$$m_G = \frac{P_c V_f}{r T_c} \quad (12)$$

where,

$$\varphi(\gamma) = \left(\frac{2}{\gamma + 1} \right)^{\frac{1}{\gamma - 1}} \left(\frac{2}{\gamma + 1} \right)^{0.5}$$

and mass emission of gases $\dot{m}_e = S u \rho_P$ (13)

During the first period, the pressure reaches its maximum value so rapidly that the chamber free volume V_f and the burning surface S do not change much and their values can be assumed to be equal to the initial values V_{f0}, S_0 then,

$$\frac{dP_c}{dt} = \frac{1}{V_{f0}} [C_1 P_c^\alpha K_E (\rho_P - \frac{P_c}{r T_c}) - C_2 P_c] \quad (14)$$

where,

$$C_1 = X^T T_c S_0 u_0 f(T_P),$$

$$C_2 = \varphi(\gamma) A_C (r T_c)^{0.5}$$

B. Second period

This part of pressure time curve starts after the pressure peak till the end of burning. The burning surface, chamber free volume and burning thickness all change with time according to equations (2),(3) and (7), so that the differential equation describing this part is,

$$\frac{dP_c}{dt} = \frac{1}{V_{f0} + C_3 P_c^\alpha K_E t (1 - C_4 P_c^\alpha K_E t)} \quad (15)$$

$$[C_1 P_c^\alpha K_E (1 - 2C_4 P_c^\alpha K_E t) (\rho_p - \frac{P_c}{r T_c}) - C_2 P_c]$$

where,

$$C_3 = S_0 u_0 f(T_p),$$

$$C_4 = \frac{a_i}{2} u_0 f(T_p)$$

Differential equation (15) also describes the pressure course from the starting of rocket motor function till the end of burning according to initial conditions.

Differential equation (14) is solved using the atmospheric pressure and zero time as initial conditions. When the pressure reaches its maximum value, the differential equation (15) completes the course of pressure using the last values of pressure and time obtained from equation (14) as initial conditions.

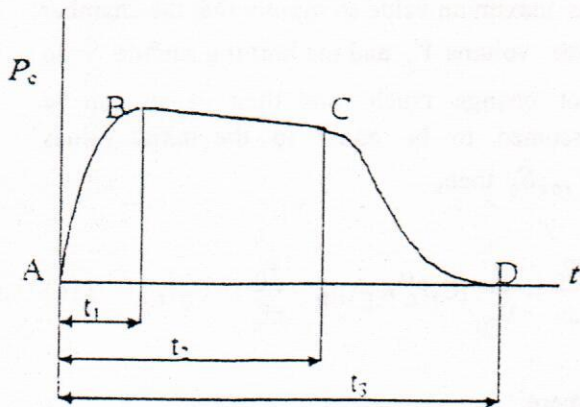


Fig. (1)

Calculation of Results

As an application for the theory introduced, a propellant of colloidal type and of grain shape has been used, where: $\gamma = 1.28$, $\chi = .98$, $T_c = 2230$ K, $r = 372.999$ J kg K⁻¹, $P_E = 8$ MPa, $\varphi_V = 1.2$, $\xi_K = 1.15$, $D = .63$ m, $D_1 = .055$ m, $D_2 = .049$ m, $D_3 = .012$ m, $L_p = .16$ m and assume $T_p = T_N = 15^\circ$.

The necessary algorithm for solution is,

$$K_r = \frac{D_2^2 - D_3^2}{D_1^2}$$

$$\bar{\theta} = \frac{D_1}{D}$$

$$A_{r0} = \frac{\pi}{4} D^2 \bar{\theta} (1 - K_r)$$

$$S_0 = N_T \pi (D_2 + D_3) [L_p + \frac{D_2 - D_3}{2}]$$

$$u_0 = \frac{u}{P_E^\alpha}$$

$$K_s = \frac{P_E^{1-\alpha} \varphi(\gamma)}{(r T_c)^{0.5} \rho_p u_0} \quad (16)$$

$$t_b = \frac{D_2 - D_3}{4 u_0 P_E^\alpha}$$

$$A_c = \frac{S_0}{K_s}$$

$$V_{r0} = \frac{\pi}{4} \varphi_V \xi_K D^3 \bar{\theta}^2 (1 - K_r) K_L$$

$$a_1 = \frac{4 \pi (D_2 + D_3)}{S_0}$$

also the constants C_1, C_2, C_3, C_4 and differential equations (14) and (15).

The used ranges of parameters are:

$$K_E (1 - 1.3)$$

$$u (.01 - .05) \text{ ms}^{-1}$$

$$\alpha (.2 - .8)$$

$$\rho_p = 1600 \text{ kg m}^{-3}$$

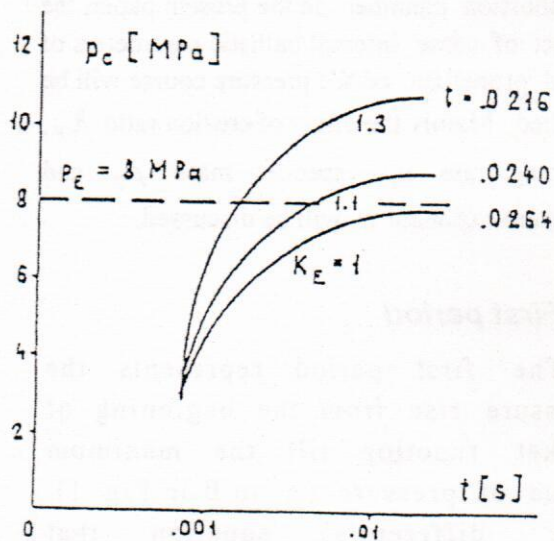


Fig. (2) Initial pressure rise for $u=0.01$, $\alpha=0.2$, $\rho_p=1600$

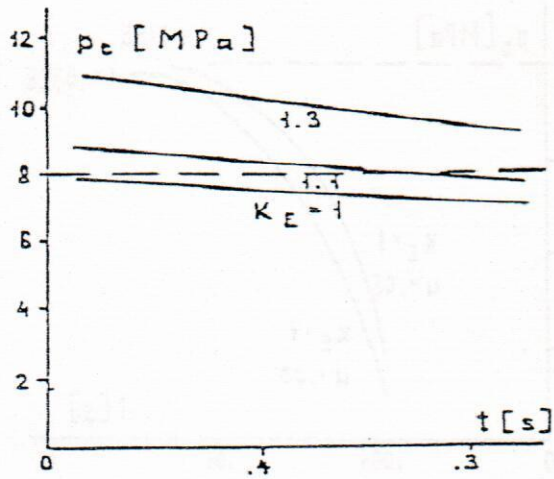


Fig. (3) Stabilization and equilibrium pressure

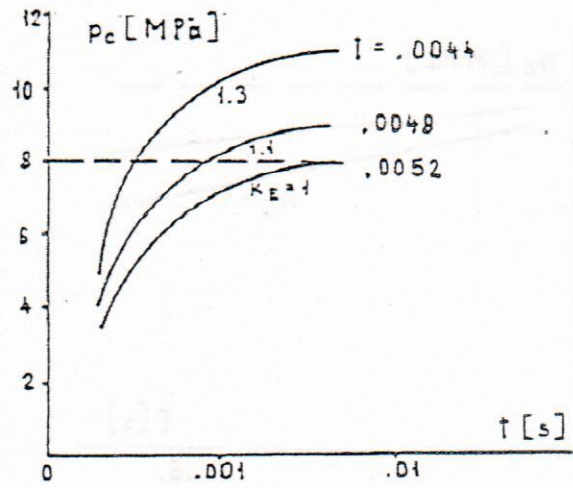


Fig. (6) Initial pressure rise $u=0.05, \alpha=0.2, \rho_p=1600$

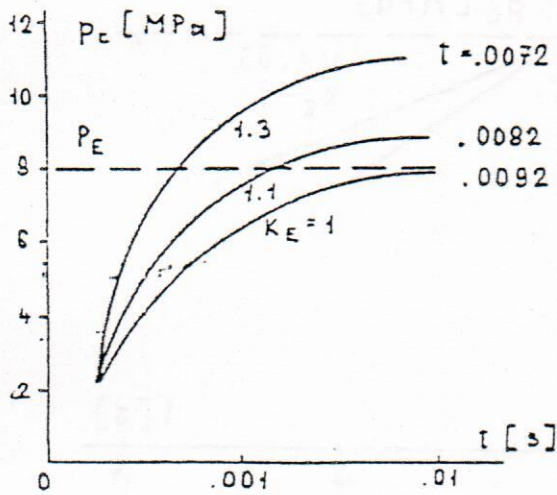


Fig. (4) Initial pressure rise for $u=0.03, \alpha=0.2, \rho_p=1600$

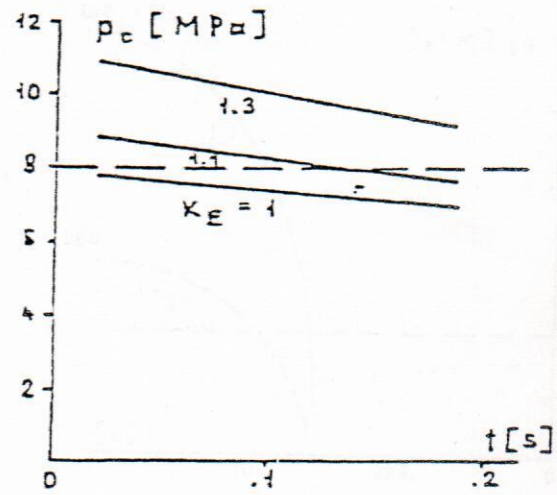


Fig. (7) Stabilization and equilibrium pressure

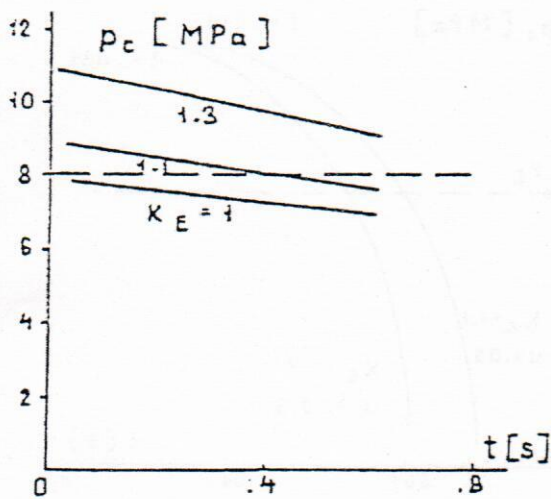


Fig. (5) Stabilization and equilibrium of pressure

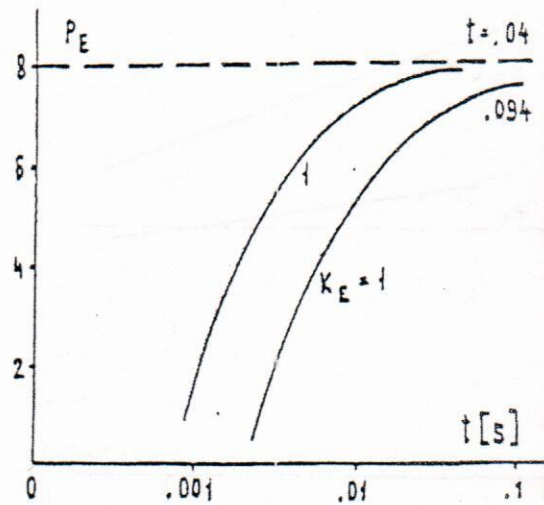


Fig. (8) Initial pressure rise for $u=0.01, \alpha=0.5, \rho_p=1600$

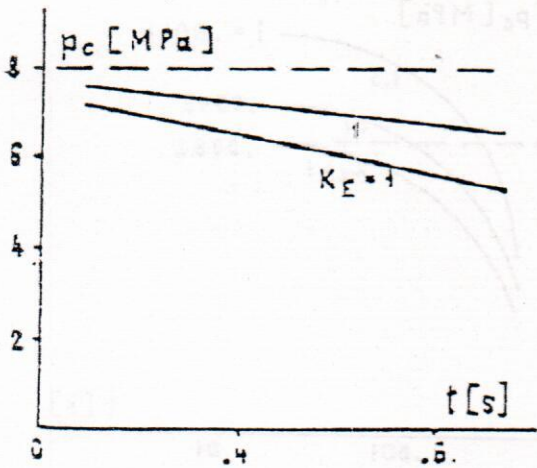


Fig. (9) Stabilization and equilibrium of pressure

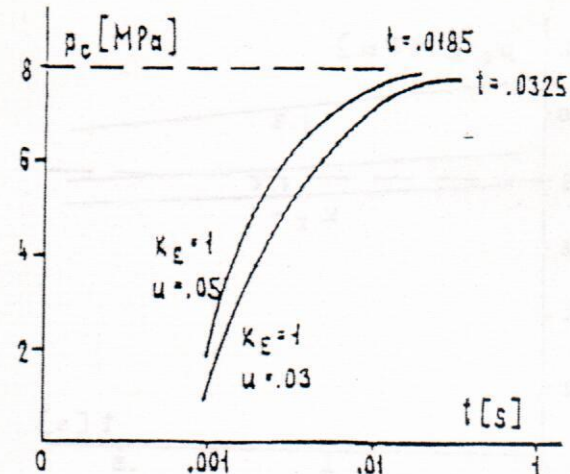


Fig. (12) Initial pressure rise for $\alpha=0.8, \rho_p=1600$

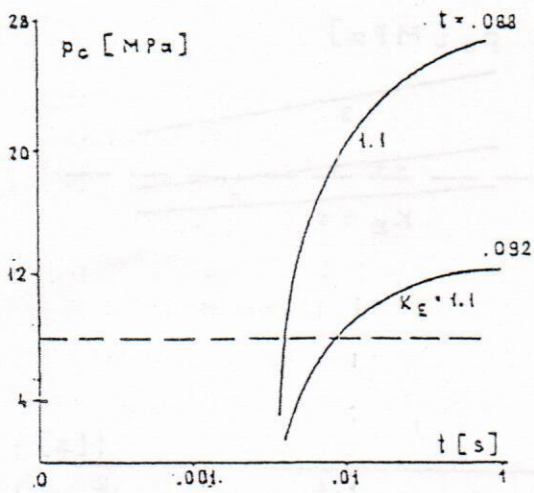


Fig. (10) Initial pressure rise for $u=0.01, \alpha=0.5, \rho_p=1600$

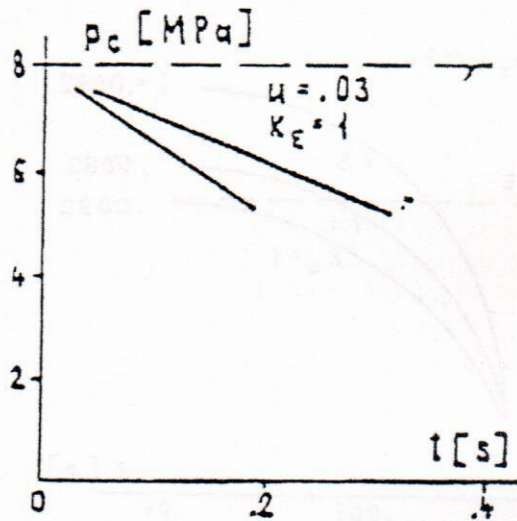


Fig. (13) Stabilization and equilibrium of pressure

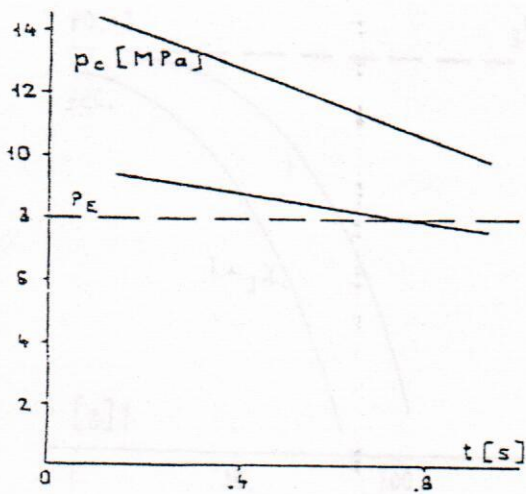


Fig. (11) Stabilization and equilibrium of pressure

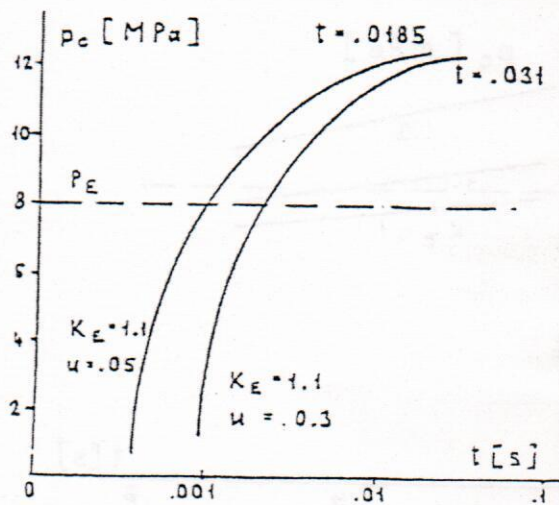


Fig. (14) Initial pressure rise for $\alpha=0.5, \rho_p=1600$

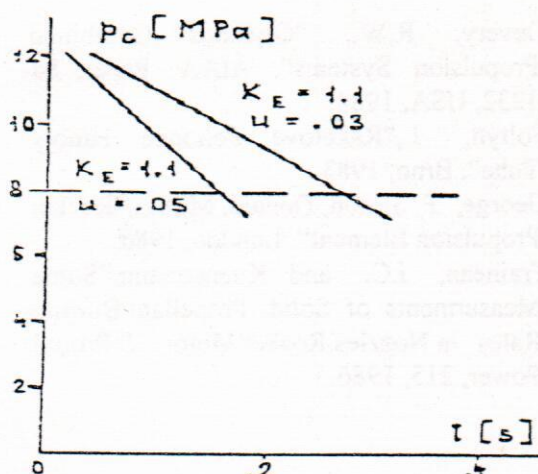


Fig. (15) Stabilization and equilibrium of pressure

CONCLUSIONS

Erosive burning takes place in each rocket motor regarding the type of propellant used, grain configuration, dimensions of grain, ratio of port area to nozzle critical area when this ratio is less than 2 and other factors. According to this it must be taken into consideration in theoretical work, otherwise it will cause difference between experimental and theoretical solution, mainly in pressure evaluation.

Through the previous calculations, the erosive phenomena have been taken into consideration with certain range. The effect of erosivity was clearly evident from results obtained. The time to reach the maximum pressure decreases with increase of erosive burning effect for certain values of u, α and ρ_p . As the burning rate u increases within presupposed range, the time to reach the same maximum pressure is shorter. This leads to early pseudo-equilibrium state and early diminishing of the erosive effect.

The effect of pressure exponent $\alpha < 1$ in combination with erosive burning and burning rate gives higher erosive peak through longer time, also longer time to pseudo-equilibrium state.

From the previous conclusion one can point out that the erosive effect can be partially controlled by choosing suitable values of the mentioned internal ballistics, then to determine accurately the performance and the structural resistance of rocket motor.

NOMENCLATURE

A_c	- nozzle critical area	$[m^2]$
A_{f0}	- initial free area	$[m^2]$
D	- rocket outer diameter	$[m]$
D_1	- rocket inner diameter	$[m]$
D_2	- grain outer diameter	$[m]$
D_3	- grain inner diameter	$[m]$
e	- burning thickness	$[m]$
K_E	- erosion ratio	$[-]$
K_f	- filling coefficient	$[-]$
K_L	- slenderness ratio	$[-]$
K_T	- temperature sensitivity	
	coefficient of solid propellant	$[C^{-1}]$
N_T	- number of grains	$[-]$
P_c	- combustion chamber pressure	$[Pa]$
P_E	- equilibrium pressure	$[Pa]$
S	- instantaneous burning surface	$[m^2]$
S_0	- initial burning surface	$[m^2]$
T_N	- normal temperature of solid propellant	$[C]$
T_c	- combustion chamber temperature	$[C]$
T_p	- temperature of solid propellant	$[C]$
t_b	- time of solid propellant burning	$[s]$
u	- burning rate of solid propellant	$[ms^{-1}]$
u_N	- nonerosive burning rate	$[ms^{-1}]$
u_0	- burning rate at unit pressure	$[ms^{-1}Pa^{-\alpha}]$
V_f	- instantaneous combustion chamber free volume	$[m^3]$
V_{f0}	- initial combustion chamber free volume	$[m^3]$
α	- exponent of burning rate	$[-]$
χ	- coefficient of thermal losses	$[-]$
γ	- adiabatic exponent	$[-]$
$\bar{\theta}$	- modified strength factor	$[-]$
ρ_p	- specific mass of solid propellant	$[kgm^{-3}]$

REFERENCES

1. Ludvik, F., Kozak, A., Svoboda, O., "Rakety, cast 1", Brno, 1982.
2. Youfang, C., "Combustion Mechanism of Double-Base Propellants with Lead

- Burning Rate Catalysts Propellants", Explosive, Pyrotechnics, 12,209-214, Weinhiem, 1987.
3. Williams, F.A., Barrere, M. and Hung, N.C., "Fundamental Aspect of Solid Propellant Rockets", England, 1969.
 4. Kamath, H., Arora, R. and Kuo, K.K., "Erosive Burning Measurements and Prediction for a Highly Aluminized Solid Propellant", AIAA Paper, 82-1111, USA, 1982.
 5. Devery, R.W., "Olympus Combined Propulsion Systems", AIAA Paper, 84-1232, USA, 1984.
 6. Foltyn, J., "Raketove Pohonne - Hmoty Tuhe", Brno, 1983.
 7. George, P. Sutton, Donald, M.ross, "Rocket Propulsion Element", London, 1988.
 8. Trainean, J.C. and Kuentzmann, "Some Measurements of Solid Propellant Burning Rates in Nozzles Rocket Motor", J. Propul. Power, 215, 1986.